15th Australasian Fluid Mechanics Conference
The University of Sydney, Sydney, Australia
13-17 December 2004

# Transient Behaviour of the Fuel Spray from an Air-Assisted, Direct Fuel Injector

**S.H. Jin[1], M.J. Brear[1], G. Zakis[1], H.C. Watson[1] and C. Zavier[2]**

[1]Department of Mechanical and Manufacturing Engineering
University of Melbourne, VIC, 3010 AUSTRALIA

[2]Orbital Engine Company (Australia) Pty. Ltd.
Balcatta, Western Australia, 6021 AUSTRALIA

## Abstract

The transient behaviour of the fuel spray from an air-assisted fuel injector in a constant volume chamber has been investigated experimentally. The relative Sauter mean diameter (SMD) of the spray droplets was determined using planar laser induced fluorescence (PLIF) and planar Mie scattering. Planar images of the ensemble averaged relative SMD with various injection conditions were obtained by calculating the ratio between the two laser light intensities at a given point. The penetration length and the spray shape factor were also obtained. The ensemble averaged results suggest the existence of vortices that are shed from the injector tip, and which entrain the smaller droplets. Results also show that the characteristics of the injector vary weakly with several particular injection parameters, notably the fuel injection pressure and the delay between fuel and air injection.

## Introduction

In order to meet ever-tightening emissions regulations whilst simultaneously minimising fuel consumption and $CO_2$ emissions, many efforts have been made recently to improve the performance of gasoline fuelled spark ignition engines. Such efforts include the manipulation of in-cylinder flow, optimisation of the electronic control systems, and optimisation of direct injected spark ignition (DISI) fuel systems [1,2]. The improvements in fuel economy obtained by using DISI have prompted an increased adoption of this technology in passenger vehicles. Further study of fuel sprays in SI engines aims in particular to minimise the emissions of hydrocarbons (HC), oxides of nitrogen ($NO_x$) and particulate matter (PM) and improve efficiency through more complete combustion. Since the fuel injection pressure of a DISI engine is typically lower than that of a diesel engine, larger fuel droplets can exist in the cylinder, and so poor fuel distribution and slow evaporation may result. This is particularly the case during cold engine starting and warm-up, when the highest levels of HC emissions over the entire drive-cycle usually occur. For these reasons, air-assisted direct injectors with improved fuel atomisation are currently under development.

The air-assisted direct injection fuel system has many unique features compared with single fluid systems. The most obvious difference is the addition of air, which is injected directly into the combustion chamber with the fuel. The pressure and quantity of the air influence the characteristics of spray. The characteristics of the fuel spray play an important role in mixture preparation, which has an effect on combustion and emissions, so it is important to understand the spray characteristics within the combustion chamber.

The droplet diameter of the spray is one of the most important aspects of spray characteristics. Laser diffraction particle analysis (LDPA) and phase Doppler particle analysis (PDPA) are generally used to measure the droplet size, but there are disadvantages to both methods. LDPA is not suitable for dense spray measurement because of multiple diffraction phenomena, and PDPA is used for point measurement, so it needs a great deal of time and effort to obtain the droplet size distribution across the whole spray. It is therefore worthwhile developing alternative methods, such as the present, planar imaging technique using a laser sheet, to study the transient spray characteristics [3-5].

This paper presents an experimental study of an air-assisted, direct injection (DISI) system. The technique of 'laser sheet drop-sizing' (LSD) is used to examine the transient behaviour of the fuel spray. These results are compared to back-illuminated images at the same conditions, and the spray-tip penetration and shape factor are also determined.

## Experimental methods

The Sauter mean diameter (SMD) can be determined for liquid droplets by combining the well established techniques of Mie scattering and laser induced fluorescence (LIF). The intensity of the fluorescence signal measured by LIF is proportional to the concentration of the fluorescing molecules. As such, the observed fluorescence originates almost entirely from molecules in the liquid phase. As shown in equation (1), the fluorescence intensity per unit area $I_{LIF}$ of the emitted light is *ideally* proportional to the cube of the particle diameter, assuming negligible light absorption and negligible optical amplification [4].

$$I_{LIF} = C_1 I_0 e^{-kx} \int_0^\infty D^3 \frac{dn}{dD} dD, \qquad (1)$$

where $I_o$ is the intensity of the incident laser beam, $x$ is the distance travelled by the incident laser beam, $k$ is an attenuation factor, $D$ is the droplet diameter, $dn$ is the droplet number density between $D$ and $D+dD$ and $C_1$ is a constant that depends on the experimental configuration. In the case of significant absorption or optical amplification, $I_{LIF}$ has been observed to vary with particle diameter to a power varying between 2.4 and 3.1 [4]. The exact relationship can only established by examining a range of droplets of known diameter, and the ideal cubic relationship for the fluorescence is therefore assumed.

According to Lorenz–Mie theory, the intensity of Mie scattering is a function of droplet diameter, the reflection rate of the droplet, polarization, and the wavelength of the incident beam. In the case of spherical droplets with a diameter larger than 1μm and illuminated with a beam of wavelength 355nm, the intensity is approximately proportional to the square of droplet diameter [4], and can be expressed as:

$$I_{Mie} = C_2 I_0 e^{-kx} Q_{sca} \int_0^\infty D^2 \frac{dn}{dD} dD, \qquad (2)$$

where $C_2$ is a coefficient determined by the characteristics of the detecting optical system and $Q_{sca}$ is related to the angle between the direction of incident laser beam and the detecting direction. Using equations (1) and (2), it is then found that the SMD is proportional to the ratio between the LIF and Mie intensities:

$$\frac{I_{LIF}}{I_{Mie}} = \frac{C_1}{C_2 Q_{sca}} \frac{\int_0^\infty D^3 dn}{\int_0^\infty D^2 dn} = \frac{D_{32}}{C}, \qquad (3)$$

where $C=C_2Q_{sca}/C_1$ has the units of length and could be determined with an appropriate calibration method, such as laser diffraction particle analysis (LDPA) or phase Doppler particle analysis (PDPA) [6]. The simultaneous measurement of the LIF and Mie scattering signals also yields a relative SMD of the spray that is not related to the intensity of the incident laser sheet or the absorption of the laser sheet.

## Experimental layout

A schematic of the experimental set-up is shown in figure 1. The light source used was a Nd:YAG laser (Quantel, TwinsB). The laser pulse duration was 5ns and the maximum energy was 120mJ at a wavelength of 355nm. A sheet beam was formed using a set of cylindrical lenses and the optical system was carefully aligned to minimize unwanted stray light such as reflections from the chamber wall. The fluorescence and Mie scattered signals were imaged at a right angle to the laser beam using an ICCD camera (LaVision, FlowMaster3 with intensifier) with a UV Nikon lens (f/# 4.5) and a gate width of 100ns. A GG-400 Schott glass filter was used for the fluorescence signal and a 355nm band-pass filter for Mie scattering. Images of the LIF and Mie scattering at a given instant during subsequent injection events were ensemble averaged. The ensemble averaged distributions obtained using 100 and 1000 ensemble averages were very similar, so all the results presented in this paper used 100 ensemble averages.

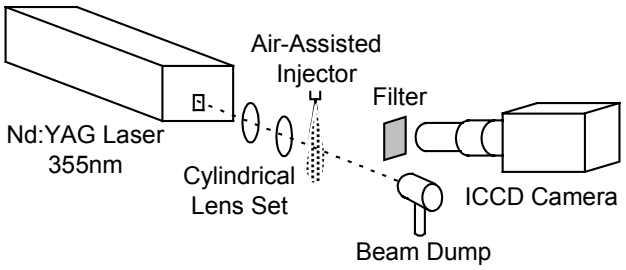


Figure 1. Schematic of experimental set-up.

Standard, unleaded petrol (ULP) with an octane number of 91 was used as the fuel during experiments. The LIF spectrum of this particular ULP blend is broadband, and ranges from 380nm to 440nm, with a peak at 405nm. Absorption and emission bands are spectrally well separated, ensuring the absence of fluorescence trapping and making possible the separation of the Mie scattered and the fluorescence signals.

The air-assisted injection system comprises two main components: a fuel metering injector, similar to a port fuel injector, and an air injector, which delivers a mixture of metered fuel and air into the combustion chamber (figure 2a). The fuel injector delivers fuel into a reservoir that is internal to the injector. The air injector then delivers this (metered) fuel into the combustion chamber. This system has been reported previously to exhibit the favourable quality of small fuel droplet size [7]. A unique feature of the system is the decoupling of the direct injection event with the fuel-metering event (figure 2c). This allows the direct injection event to be tailored to the combustion requirements, rather than being limited by also needing to perform the fuel metering, as is the case in high-pressure single fluid injection systems. The air-assisted injection system, installed in the constant volume chamber, has the capability of varying the chamber pressure and uses a nominal injection air pressure of 650kPag and a fuel pressure of either 720 or 800kPag. Both fuel and air injection pressures were controlled by adjusting pressure regulators. Table 1 outlines the experimental conditions of the air-assisted fuel injector. With a fuel injection duration of 4.1ms at 720kPa fuel pressure and 3.1ms at 800kPa, about 10mg of fuel was injected at a frequency of 1Hz. Injection timing, laser triggering and ICCD camera control were controlled by LABVIEW software. The times that are reported in this paper refer to the time after the trigger pulse was sent to the injector driver. This means that the first appearance of fuel is somewhat later due to delays within the injector driver and the mechanical properties of the injector. These unavoidable delays are typically a few hundred microseconds long and will be discussed later in the paper. The experiments were performed with the chamber at ambient temperature and pressure and quiescent gas conditions.

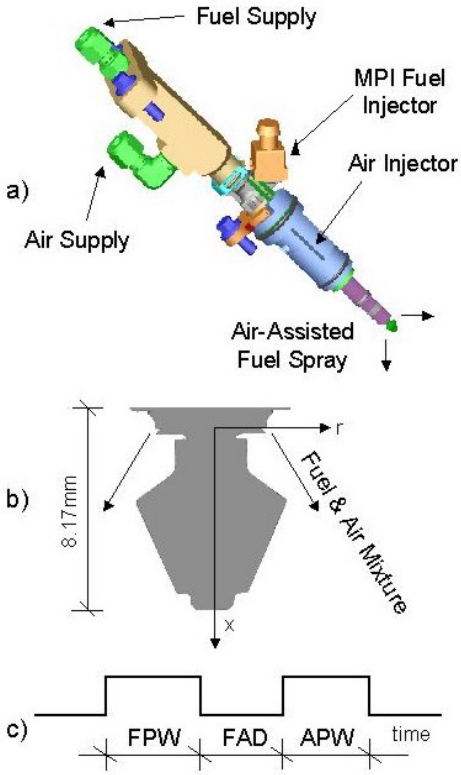


Figure 2. The air-assisted direct fuel injection system, showing a) overall configuration, b) the injector tip and c) timing schedule

| | |
|---|---|
| Fuel injection pressure (FIP) | 720 & 800kPa gauge |
| Air injection pressure (AIP) | 650kPa gauge |
| Fuel pulse width (FPW) | 4.1ms & 3.1ms |
| Air pulse width (APW) | 3ms |
| Fuel metering gain (FMG) | 10mg/pulse |
| Air metering gain (AMG) | 8.43mg/pulse |
| Fuel and air injection delay (FAD) | -1, 0 and 1ms |
| Ambient pressure | 101kPa abs. |

Table 1. Experimental conditions.

## Results and Discussion

The relative SMD of an air-assisted direct fuel injector has been measured using LIF and Mie scattering. Figure 3 shows ensemble averaged LIF, Mie scattering and relative SMD images collected separately. These images were obtained at 1.8ms after the start of air injection for 720kPa fuel injection pressure and 650kPa air injection pressure. Both LIF and Mie scattering images were not corrected for laser profile variation since the images and the profiles are divided to produce the relative SMD. The systematic laser profile features could therefore be cancelled across both the laser height and thickness of the laser sheet. The LIF image shows the liquid volume fraction, with most of the fuel mass in the centre of the spray. The Mie scattering image also has a strong signal in the centre of the spray but is narrower in width compared to the LIF image. The relative SMD image possesses a

small degree of asymmetry about the injector centreline, and such behaviour was seen throughout the present set of experiments (eg. figure 7). Previous experiments showed that similar, asymmetric results were reflected when the injector was rotated $180^0$, thus showing that this was due to non-axisymmetry in the experimental set-up, rather than in the measurement technique.

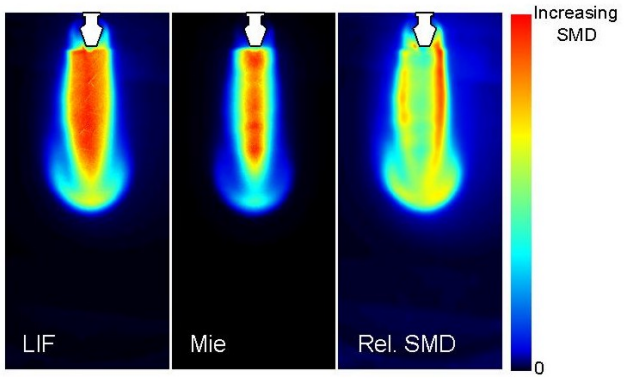


Figure 3. Time-averaged images of LIF signal (left), Mie scattering signal (middle) and relative SMD (right).

The relative SMD image shows that the edge of the spray contains larger droplets, whilst there are smaller droplets in the centre. Near the nozzle tip, the signal is not well defined due to the presence of fuel ligaments and surface scattering of the incident laser beam. Each of the three images in figure 3 shows that the spray roughly resembles a downward pointing arrow; the Mie scattered result shows this most clearly. This behaviour is thought to be due to the shedding of a vortex ring from the injector at the start of injection. Such behaviour is common in studies of pulsing, single phase injection. In the present, two phase case, the smaller droplets are presumably entrained more by the vortex ring, and are wrapped around the ring as it translates, leading to this 'arrowhead' shape. This behaviour, if true, highlights the coupling between the gas and liquid phases in this injection system, and is very different to that of a liquid-only injector. Further experiments (in particular particle image velocimetry) and ongoing numerical simulations will determine whether this vortex structure actually exists.

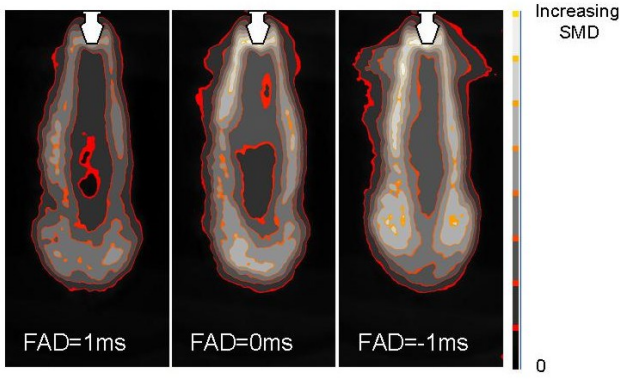


Figure 4. Comparison of relative SMD for different time interval between fuel and air injection (FAD).

Figure 4 shows the effect of fuel air delay (FAD) on the ensemble averaged SMD. These images were measured 2.0ms after the start of air injection with a 720kPa fuel injection pressure and 650kPa air injection pressure. As can be seen in this figure, there is a difference in droplet size between locations such as the centre and periphery of the spray, and the droplet size is larger away from the spray centreline. This is thought to be due to the larger droplets maintaining their initial trajectory better because of their greater inertia. The smaller droplets are deflected more by the air, and so can migrate to the injector centreline. The relative SMD also increases as the FAD decreases. Reasons for this trend in FAD are not clear, and are presently being studied using numerical simulations.

Spray characteristics of interest also include the spray tip penetration length, the spray cone angle and the overall spray SMD. The spray tip penetration length was measured directly from the spray images and obtained by measuring the distance from the injector exit (figure 2b) to the lowest intensity Mie scattering contour in the axial direction. Figure 5 shows the spray tip penetration length as a function of time for the two different fuel injection pressures (FIP) and delay between fuel and air injection (FAD). The effects of varying the FIP and FAD are relatively small. This is to be expected for positive FAD's, since the fuel and air injection events are then separate, with the fuel being dumped into the internal reservoir and then injected by the air into the chamber. The spray penetration is also expected to decrease for negative FAD's, and figure 5 shows this beginning to occur by FAD=-1ms.

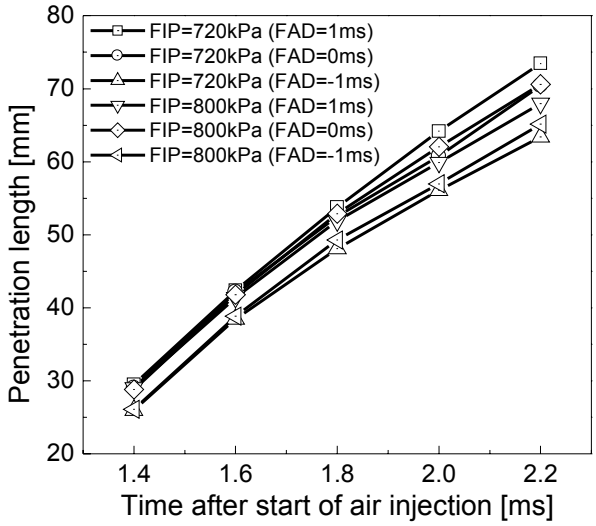


Figure 5. Spray tip penetration length for different fuel injection pressure (FIP) and time interval between fuel and air injection (FAD).

The spray shape factor is defined as

$$\text{spray shape factor} = \tan^{-1}\left(\frac{\text{maximum spray width}}{\text{spray penetration length}}\right) \quad (4)$$

Figure 6 shows that the spray shape factor decreases rapidly after the start of injection at all the conditions studied. As figure 7 shows, this is due to the width of the spray remaining relatively contained as the spray penetrates into the chamber. This highlights once again the effect of the air-assist on the spray development [7].

Figure 7 displays a collection of back-illuminated and relative SMD spray images for different times after the start of air injection. The relative SMD results for later times are not shown due to the charge impinging on the chamber walls and filling the chamber. As mentioned earlier, there is a delay between the electrical triggering of the start and end of injection and the mechanical response of the injector. The opening and closing delays for this injector were approximately 1.0ms and 0.6ms respectively. The back-illumination passes through the entire spray and is therefore a projection of an (ideally) axisymmetric problem, rather than a planar image such as those shown for the relative SMD. Nonetheless, the penetration of the spray in both

cases is similar, and there is some suggestion of the aforementioned spray 'arrowhead' in the back-illuminated results at 1.8ms.

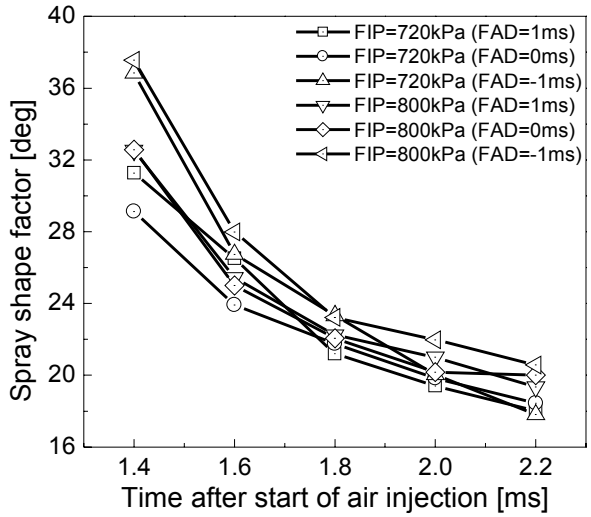


Figure 6. Spray shape factor for different fuel injection pressure (FIP) and time interval between fuel and air injection (FAD).

## Conclusions

The characteristics of the fuel spray from an air-assisted, gasoline direct fuel injector have been performed using optical techniques. The technique of 'laser sheet drop-sizing' (LSD), which required the combined use of Mie scattering and laser induced fluorescence (LIF), allowed determination of the relative Sauter mean diameter (SMD) of the fuel spray. Both the Mie and LIF images were ensemble averaged over separate injection events, thereby permitting study of the transient development of the ensemble averaged spray.

Several, interesting aspects of the transient spray behaviour were noted. The previously reported spray containment enabled by the air-assist was observed, with the spray maintaining a narrow width as it penetrated into the chamber. The largest droplets were also observed to lie away from the spray centreline, which was considered reasonable. Finally, there was also some evidence that a vortex ring was shed from the injector at the start of injection, although further, planned experimental and numerical studies are required to confirm this.

## Acknowledgments

This work was supported by the Orbital Engine Company, Holden Limited and the Australian Research Council. The authors are particularly grateful for the strong co-operation of their industrial partners, as well as the technical support from Mr T. Grange and Mr D. Halpin.

## References

[1] Zhao, F.Q., Lai, M.C. & Harrington, D.L., The Spray Characteristics of Automotive Port Fuel Injection – A Critical Review, *SAE Paper* 950506, 1995.

[2] Sampson, M.J. & Heywood, J.B., Analysis of Fuel Behaviour in the Spark-Ignition Engine Start-Up Process, *SAE Paper* 950678, 1995.

[3] Yeh, C., Kosaka, H. & Kaminoto, T., Fluorescence / Scattering Image Technique for Particle Sizing in Unsteady Diesel Spray, *JSME Trans*., B **59**, 1993, 308-313.

[4] LeGal, P., Farrugia, N. & Greenhalgh, D.A., Laser Sheet Dropsizing of Dense Sprays, Opt. *Laser Technol*., **31**, 1999, 75-83.

[5] Stojkovic, B.C. & Sick, V., Evolution and Impingement of an Automotive Fuel Spray Investigated with Simultaneous Mie/LIF Techniques, *Appl. Phys*., B **73**, 2001, 75-83.

[6] Jermy, M.C. & Greenhalgh, D.A., Planar Dropsizing by Elastic and Fluorescence Scattering in Sprays Too Dense for Phase Doppler Measurement, *Appl. Phys*., B **71**, 2000, 703-710.

[7] Cathcart, G. & Zavier, C., Fundamental Characteristics of an Air-Assisted Direct Injection Combustion System as Applied to 4-Stroke Automotive Gasoline Engines, *SAE Paper* 2000-01-0256, SP-1499, 2000.

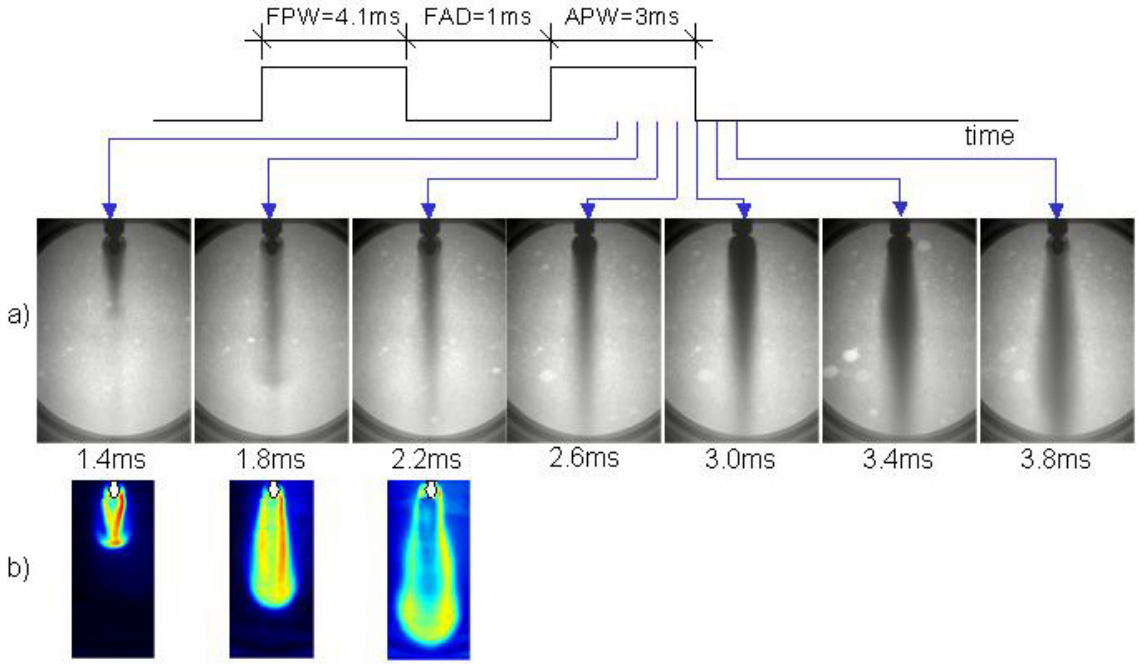


Figure 7. Spray profiles after the start of air-injection showing a) back-illumination and b) relative SMD results (key as in figure 3).